Analysis of the newly observed [15.05]$0^+ - X\,^3\Sigma^-(0^+)$ transition of WS observed using intracavity laser spectroscopy with Fourier-transform detection

Kristin N. Bales,[1] Jack C. Harms,[1] James J. O'Brien,[1] and Leah C. O'Brien[2,a)]

AFFILLIATIONS

[1]*Department of Chemistry and Biochemistry, University of Missouri – St. Louis, Saint Louis, MO 63121, USA*

[2]*Department of Chemistry, Southern Illinois University Edwardsville, Edwardsville, IL 62026, USA*

[a)]Author to whom correspondence should be addressed: lobrien@siue.edu

ABSTRACT

Several bands in a new electronic transition of tungsten sulfide, WS, have been recorded at Doppler-limited resolution using intracavity laser spectroscopy with Fourier-transform detection (ILS-FTS). WS molecules were produced in the plasma discharge of a W-lined Cu hollow cathode in the presence of a gas mixture containing approximately 70% Ar and 30% H_2, with a trace amount of CS_2 at a total pressure of 1 torr. The (0,0), (1,0), (2,0), (1,1), (2,1), and (3,1) bands of the [15.05]$0^+ - X\,^3\Sigma^-(0^+)$ transition of WS were observed. Line positions for the four major isotopologues ($^{182}W^{32}S$, $^{183}W^{32}S$, $^{184}W^{32}S$, and $^{186}W^{32}S$) of the (0,0), (1,0), and (2,0) bands were used in the fit. The WS bands were analyzed using PGOPHER, with previously determined constants for the $X\,^3\Sigma^-(0^+)$ ground state [Harms *et al.*, *J. Mol. Spectrosc.* **374**, 111378 (2020)] held fixed in the fit. A perturbation was observed in the (0,0) band which appears to be caused by an electronic state that has not been observed. Molecular parameters for the newly identified excited state are presented.

I. INTRODUCTION

The electronic structure of tungsten monosulfide, WS, has become a focus of both theoretical and spectroscopic interest. Tungsten disulfide, WS_2, has been investigated as a thin film semiconductor for use in nanoelectronic devices[1] and as a window layer in solar cells, with potential to provide a low cost, non-toxic photovoltaic material.[2] A growing body of work has begun to elucidate more details of the very complex electronic structure of the W-S bond that results from the large number of unpaired electrons and accessible valence orbitals. Density functional theory (DFT) calculations were performed in 2002 by Liang and Andrews.[3] In 2019, Tsang *et al.*[4] provided a more thorough look at WS with high-level *ab initio* calculations, experimental observations using laser induced fluorescence (LIF), and analyses of several transitions. Also in 2019, Zhang *et al*.[5] used LIF to investigate spin-spin splitting in the $^3\Sigma^-(0^+)$ ground state. Our lab has published two recent papers (Harms *et al*.[6,7]) that report the observation of new electronic transitions that connect to the $X\,^3\Sigma^-(0^+)$ ground state. Our more recent paper on the $[14.26]0^+ - X\,^3\Sigma^-(0^+)$ transition[7] incorporated intracavity laser spectroscopy with Fourier-transform detection (ILS-FTS) data from previous work in our lab[6] as well as LIF data from two transitions observed by Tsang *et al*.[4] to conduct a comprehensive fit of the data to a mass-independent Dunham model[8] to characterize the ground state. Most recently, a paper by Zhang *et al.*[9] reported the identification of seven low-lying Ω states observed by dispersed fluorescence, and included the rotational analysis of the (0,0) bands of additional electronic transitions observed using LIF. Some transitions observed strongly in the LIF spectrum were "quasi-forbidden" by the computational model implemented by Tsang *et al.,*[4] motivating a reexamination of the relativistic corrections to hopefully bring theory and experiment into closer alignment.[9] The spin-orbit matrix was calculated at a higher level of theory, and transition dipole moments (TDMs) were calculated from the resulting Hund's Case (c) Ω-states. These TDMs were used to correlate the experimental electronic states observed by LIF to the *ab initio* Ω-states, providing some insight into the underlying Λ-S character of those spectroscopic states.

In this work, we have observed several new vibrational bands of a new electronic transition of WS using intracavity laser spectroscopy with high-resolution Fourier transform detection (ILS-FTS). Three bands were analyzed and identified as the (0,0), (1,0), and (2,0), bands of the $[15.05]0^+ - X\,^3\Sigma^-(0^+)$ transition. The determined molecular constants are presented here.

II. EXPERIMENTAL METHODS

The spectra used for analysis were collected in the visible region (14,985 – 16,100 cm^{-1}) using the ILS-FTS system at the University of Missouri – St. Louis, which has been previously described in detail.[10] The ILS component used DCM laser dye. WS molecules were produced within the resonator cavity in a plasma discharge created when a radio frequency-pulsed DC current of 0.50 – 0.60 A or a DC current of 0.05 – 0.15 A was applied by our ENI RPG50 Pulsed DC plasma generator (now MKS RPDG 5kW pulsed DC Plasma Generator) to a 25 mm long tungsten-lined copper hollow cathode. An estimated plasma temperature of 500 K and a molecular mass of 216 amu ($^{184}W^{32}S$) predicts a full width half maximum (FWHM) Doppler linewidth of 0.017 cm^{-1}.[11] The total pressure within the reaction chamber was approximately 1 torr attained by gas flows of approximately 70% Ar and 30% H_2, with a trace of CS_2, regulated by three mass flow controllers.

In the ILS-FTS method, the entire broadband laser profile of the ILS laser is directed into a Bruker IFS 125 M FTS. The laser profile is approximately Gaussian with a baseline width ranging from 20 to 100 cm^{-1}, depending on the ILS gain medium (about ~40 cm^{-1} for this data). When the power supply is in operation, molecular absorption due to species produced in the plasma becomes superimposed upon the broadband profile of the ILS laser – this laser profile is termed the "plasma spectrum." The plasma is maintained while the moving mirror of the FTS system is scanned – often, several scanned interferograms are coadded prior to FT. The FTS is controlled using OPUS (v.8.5.29), the software provided by Bruker. For this study, spectra were acquired at a resolution of 0.01 cm^{-1} and 4-6 scans of the FT spectrometer were coadded to produce each spectrum. Acquisition of each ~40 cm^{-1} wide plasma spectrum was followed by collection of a background spectrum with identical instrument settings. The two spectra were divided using the spectrum calculator function in OPUS, and only the most intense central portion (~20 cm^{-1}) of each Gaussian laser output profile was used.

As a technique with forward and backward traveling laser beams, the ILS technique is capable of sub-Doppler resolution via Lamb dips as shown by Baev et al.[12,13] However, Lamb Dip spectroscopy is based on a saturation condition (Demtröder[14]) and requires a configuration that can resolve the very narrow Lamb dip at the center of each Doppler-limited peak. Resolving the Lamb dip can be achieved by using either a narrow, scanning excitation source (i.e., ring dye-laser) or a detector system with sufficient resolution (monochromator or FTS with resolution element on the order of ~0.004 cm^{-1}). This electronic transition of WS is rather weak with average T% > 50 for our spectra, and thus the saturation condition is not achieved.

Six rotational bands were identified in the region investigated that have been assigned to the (2,0), (3,1), (1,0), (2,1), (0,0), and (1,1) bands of the $[15.05]0^+ - X\,^3\Sigma^-(0^+)$ transition of WS. Each band spanned ~100 cm^{-1} (~5 adjacent/overlapping ILS profiles) before signal-to-noise became too low to provide additional insight. Power supply and ILS settings were optimized for each band system prior to collection. While the alteration of conditions prevents direct comparison of relative intensity, the (0,0) band was the strongest of those studied, appearing at very "gentle" discharge conditions (50 mA DC) and short generation times (effective pathlength, L_{eff}<200 m). The (1,0) band was slightly weaker, requiring a higher current discharge, and the (2,0) band was significantly weaker than the other two, requiring both a longer generation time (L_{eff}~500 m), as well as a higher current. For the (2,0) band, all plasma spectra and all background spectra were added together before division to enhance the signal-to-noise ratio. Using PGOPHER,[15] a smooth baseline correction was applied to compensate for any shift in laser profile position between collection of plasma and background spectra. Each baseline-corrected spectrum was converted to an absorbance spectrum. The spectra were calibrated to an accuracy of 0.001 cm^{-1} using observed Ar I line positions reported by Kerber *et al*.[16] The (0,0), (1,0), and (2,0) bands were then rotationally analyzed using PGOPHER,[15] with a total of 1,118 lines included in the fit. Molecular constants determined by Harms *et al*.[7] for the ground state were used and held fixed in the fit.

III. **RESULTS AND DISCUSSION**

Three prominent, red-degraded bands were observed in the visible region at Doppler-limited resolution. The bandheads appeared at approximately 15,051, 15,574, and 16,093 cm^{-1}, and were

analyzed and identified, respectively, as the (0,0), (1,0), and (2,0) bands of the [15.05]$0^+ - X\,^3\Sigma^-$ (0^+) transition of WS. Weaker bandheads were observed 33 – 40 cm^{-1} to the red of each of the main bandheads, appearing at 15,018, 15,537, and 16,053 cm^{-1}, and were identified as the (1,1), (2,1), and (3,1) bands. These bands were not rotationally analyzed as they were significantly weaker and obscured by overlapping lines of the stronger bands. The (1,1) band was considerably weaker than both the (2,1) and (3,1) bands, which were quite strong. A strong vibrational progression generally indicates a change in bond length upon excitation.

Each band consisted of one P- and one R-branch for each of the four prominent isotopologues, $^{182}W^{32}S$, $^{183}W^{32}S$, $^{184}W^{32}S$, and $^{186}W^{32}S$, as illustrated in **Figure 1.** The lack of an observable Q-branch indicates the transition is of $\Delta\Omega=0$ symmetry. Combination differences confirmed the lower state is the previously observed $X\,^3\Sigma^-(0^+)$ ground state of WS, and thus the new [15.05] excited state of WS conclusively is assigned to be of $\Omega=0^+$ symmetry. At low J, the vibrational separation of isotopologues is fairly consistent with what is expected to be seen for the (0,0), (1,0), and (2,0) bands. The clear isotope separation in the P-branch of the (0,0) band is illustrated in **Figure 2**.

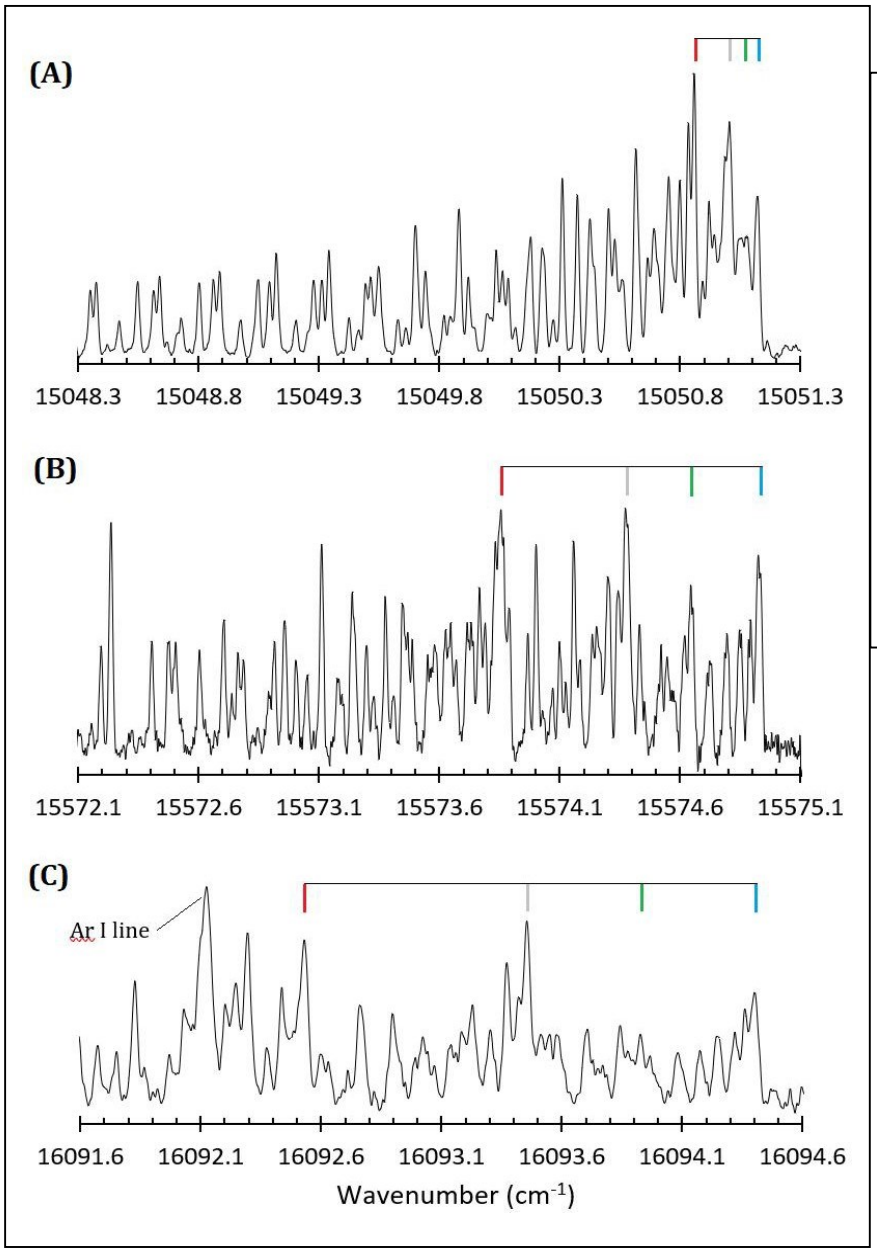

Figure 1. Bandhead positions of the $^{182}W^{32}S$, $^{183}W^{32}S$, $^{184}W^{32}S$, and $^{186}W^{32}S$ isotopologues, shown by the upper color-coded tie lines, highlighting the vibrational shifts observed in **A** (0,0) band, **B** (1,0) band, and **C** (2,0) band. Energy differences between the $^{182}W^{32}S$ and $^{186}W^{32}S$ bandheads for the (0,0), (1,0), and (2,0) bands are 0.262, 1.076, and 1.873 cm^{-1}, respectively.

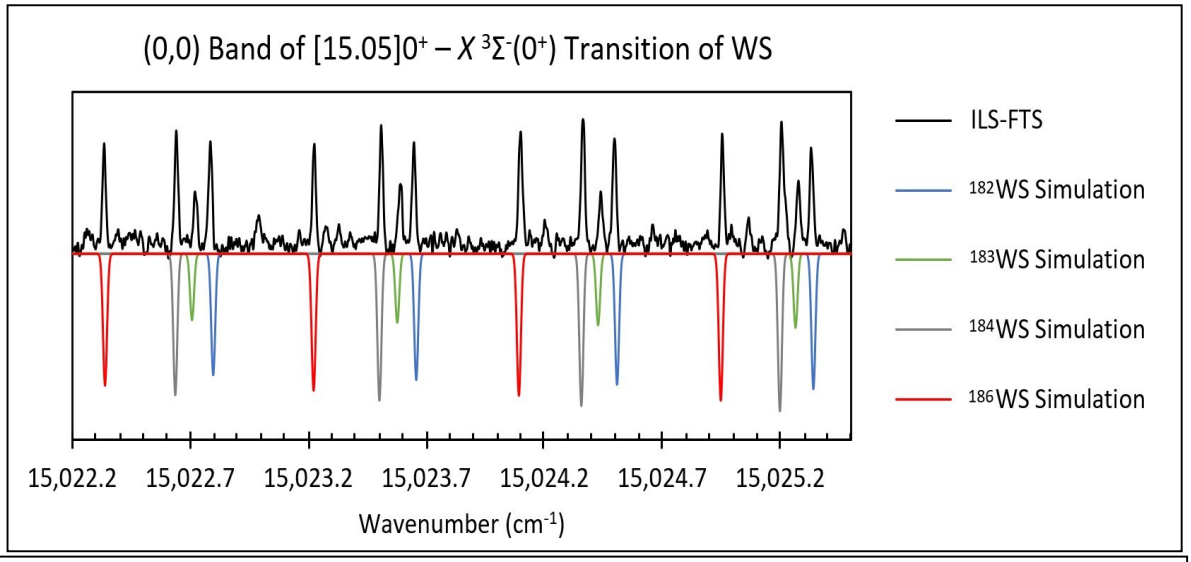

Figure 2. Illustration of clear separation of $^{182}W^{32}S$, $^{183}W^{32}S$, $^{184}W^{32}S$, and $^{186}W^{32}S$ isotopologues in the (0,0) band of the $[15.05]0^+ - X\,^3\Sigma^-(0^+)$ transition of WS. Lines shown are P-branch lines with J = 41-44 (from right to left).

Lines with J values up to ~80 were identified for many branches. A significant perturbation was seen at high J in the (0,0) band. The perturbation is strongly J dependent and mass dependent. For example, the perturbation appears at much lower J for the $^{186}W^{32}S$ isotopologue (J~45) than for the $^{182}W^{32}S$ isotopologue (J~55). **Figure 3** illustrates the fit residuals (obs-calc) for the P-branches of the (0,0) band at J>40. The residuals for the R-branches show a very similar pattern. In the final fit, a H_0 parameter was included in the excited state, and higher-J lines that could not be fit were excluded.

Several inferences regarding the perturbing state can be made based on the observed spectra. Firstly, because the perturbed lines appear at lower energy than the extrapolated positions, i.e., obs-calc < 0, we know that the perturbing state is higher in energy than the $[15.05]0^+$ state. The observation of a nearby [15.07]1 state recently reported by Zhang *et al.*[9] initially was a candidate for the cause of this perturbation; however, comparison of B values shows that the new [15.07]1 state at higher-energy has a larger B value, and thus the rotational levels of the [15.07]1 and $[15.05]0^+$ states do not approach with increasing J. Secondly, the large magnitude of the perturbation and its continuation over a large number of J values indicate that the two states must have the same symmetry (homogeneous interaction) and similar electronic energies and rotational constants. Thus, the source of the perturbation must be a nearby excited Ω=0 state which has not been observed, lying slightly higher than the $[15.05]0^+$ state.

Interestingly, Ram *et al.*[17] also reported anomalous effects related to isotopologues in three transitions of tungsten monoxide (WO): $A1 - X0^+$, $B1 - X0^+$, and $C1 - X0^+$. The three WO transitions each displayed larger than expected isotope shifts in the (0,0) bands. The $C1 - X0^+$ transition also displayed J-dependent perturbations.

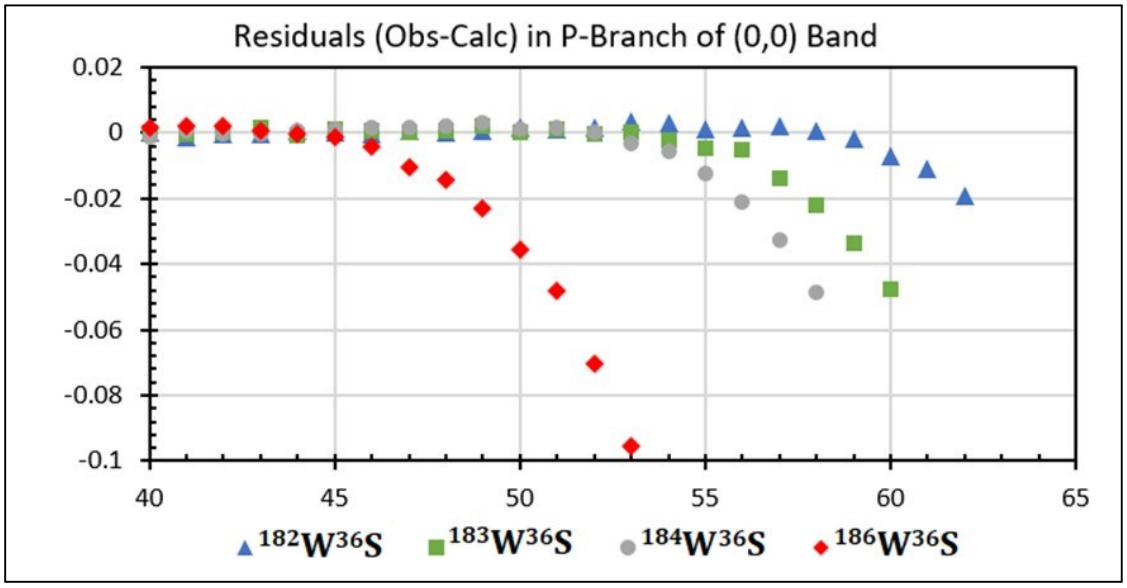

Figure 3. Fit residuals (obs-calc) for P-branches (extrapolated from J<45) of $^{182}W^{32}S$, $^{183}W^{32}S$, $^{184}W^{32}S$, and $^{186}W^{32}S$ isotopologues in the (0,0) band of the $[15.05]0^+ - X\,^3\Sigma^-(0^+)$ transition of WS.

The branches of vibrational band $[15.05]0^+ - X\,^3\Sigma^-(0^+)$ transition were fit in PGOPHER[15] as Hund's case (c) $\Omega=0^+$ states. Parameters for the $X\,^3\Sigma^-(0^+)$ ground state have been well defined and were held fixed to values given in Harms *et al.*[7] Because the (0,0) band was perturbed, a Dunham-type analysis of the excited state was not attempted. A total of 1,118 observations were fit to 40 parameters, which are given in **Table I**. The Supplementary Materials contain: the PGOPHER[15] configuration file (.pgo); the spectra in suitable format for use in PGOPHER (.ovr); the input file used to perform the fit (.lin); the output file from the final fit (.log); and a table of line positions and assignments (Table S5)

Using the molecular constants given in **Table I**, equilibrium constants for the $^{184}W^{32}S$ isotopologue were calculated, including rotational constant (B_e), bond length (r_e), term energy (T_e), vibrational constant (ω_e), and anharmonicity constant ($\omega_e x_e$). These calculated values are presented in **Table II**. The experimental results from the $^{184}W^{32}S$ isotopologue also are compared to the theoretical predictions given by Tsang *et al.*[4] (and Zhang *et al.*[9]) for their calculated $\{7\}0^+$ state, there the 7 in {} indicates that this state is the 7th *ab initio* $\Omega=0^+$ state in terms of relative energy. It is worth noting that this computational correlation contradicts Table 3 from Zhang *et al.,*[9] in which the $[17.25]0^+$ state is correlated to the $\{7\}0^+$ state. Their study of WS has been concurrent with our own, and they were unaware of the $[14.26]0^+$ and $[15.05]0^+$ states observed with ILS-FTS in our previous work[7] and this work. Simple energy ordering would suggest this reassignment, but the correlation can be further justified by examining the predicted TDMs of Zhang *et al.*[9] and the experimental transitions observed by ILS-FTS[6-7] and by LIF[4-5,9].

Table I. Molecular constants for the $[15.05]0^+$ state of WS. All values reported in cm^{-1}.

		$[15.05]0^+$			
	v	**T_v**	**B_v**	**D_v x 10^8**	**H_v x 10^{12}**
	0	15048.10327(61)	0.13838887(179)	3.422(135)	-5.068(277)
$^{182}W^{32}S$	1	15572.15326(77)	0.137821552(573)	3.3378(92)	
	2	16091.81945(44)	0.13734100(33)	3.8102(46)	
	0	15048.05587(66)	0.13826939(250)	3.849(224)	-6.290(543)
$^{183}W^{32}S$	1	15572.15789(55)	0.13781848(45)	3.2947(78)	
	2	16091.34396(69)	0.13723005(55)	3.8284(85)	
	0	15048.00716(58)	0.13813558(219)	2.964(202)	-1.2764(503)
$^{184}W^{32}S$	1	15571.60762(41)	0.13761263(31)	3.4495(47)	
	2	16090.87761(45)	0.13711769(34)	3.8083(47)	
	0	15047.88612(72)	0.13786065(358)	2.886(447)	-3.092(152)
$^{186}W^{32}S$	1	15571.08895(41)	0.13740351(34)	3.4950(56)	
	2	16089.95185(46)	0.13689934(36)	3.8433(51)	

Table II. Equilibrium constants for $^{184}W^{32}S$ determined by **this work (bold)** and by *computational prediction*[4] *(italics)*.

$^{184}W^{32}S$	B_e (cm^{-1})	r_e (Å)	T_e (cm^{-1})	ω_e (cm^{-1})	$\omega_e x_e$ (cm^{-1})
$[15.05]0^+$	**0.1384**	**2.115**	**14785**	**528**	**2.2**
$\{7\}0^{+\,a,b}$	*0.1373*[a]	*2.123*[a]	*16850*[a]	*530*[a]	*3.4*[a]

a – From Ref [4].

b – The number in {} indicates the rank of the given Ω-value (0^+), i.e., {7} is the 7^{th} 0^+ state where $\{1\}0^+$ is the lowest energy state with $\Omega=0^+$.

ILS-FTS is a direct absorption technique – ground state (or low-lying) WS molecules are excited by a single photon. This type of measurement requires a large TDM between the initial state and an excited state that occurs in the visible (or near-IR). LIF, on the other hand, is a multi-photon measurement technique – a photon is absorbed, exciting the WS molecule, then the photon is emitted and detected using a photomultiplier tube. Laser scatter precludes detection at the excitation wavelength, and cutoff filters introduce a minimum separation between the excitation energy and the detection energy of the involved photons. As such, LIF transitions are expected to be strong when an excited state has a large TDM with at least two low-lying states –

one for excitation and one for detection. This may explain why the $[15.05]0^+$ - $X\,^3\Sigma^-(0^+)$ transition was not observed by Zhang *et al.*[9]: the TDMs from the $\{1\}0^+$ ground state (in a.u.) are 0.021, 0.190, 0.122 and 0.097 to the $\{5\}0^+$, $\{6\}0^+$, $\{7\}0^+$, and $\{8\}0^+$ states, respectively. These *ab initio* states correlate most closely to the $[14.26]0^+$, $[14.76]0^+$, $[15.05]0^+$, and $[17.25]0^+$ states: transitions involving the $[14.26]0^+$ and $[15.05]0^+$ states have not been reported by LIF, but vibrational progressions involving these states and the $X\,^3\Sigma^-(0^+)$ state have now been extensively recorded using ILS-FTS. While the $\{6\}0^+$ and $\{8\}0^+$ states have TDMs of 0.208 and 0.118 a.u. to the $X\,^3\Sigma^-(1)$ state (and reasonable TDMs to the Ω sub-states of the low-lying $^5\Pi$ state), the TDMs from the $\{5\}0^+$ and $\{7\}0^+$ states are only 0.005 and 0.072 a.u. to the $X\,^3\Sigma^-(1)$ state (with negligible dipole moments to the $^5\Pi$ Ω sub-states) and would be much more difficult to observe in fluorescence.

IV. CONCLUSIONS

Six new bands of WS have been observed using ILS-FTS, and have been assigned as the (0,0), (1,0), (2,0), (1,1), (2,1), and (3,1) bands of the $[15.05]0^+ - X\,^3\Sigma^-(0^+)$ transition. Rotational analyses of the three strongest bands used Doppler-limited line positions of the four major isotopologues. The ground state constants were held fixed to those previously determined.[7] A perturbation with a large J-dependence was observed in v=0 of the new $[15.05]0^+$ state that is absent for v=1 and v=2. The new electronic state is tentatively assigned to the $\{7\}0^+$ state as calculated by Tsang *et al*.[4]

SUPPLEMENTARY MATERIALS

The Supplementary Materials contain: the PGOPHER[15] configuration file (.pgo); the spectra in suitable format for use in PGOPHER (.ovr); the input file used to perform the fit (.lin); the output file from the final fit (.log); and a table of line positions and assignments.

ACKNOWLEDGEMENTS

This work was supported by the National Science Foundation, Grant Nos. CHE-1566454 (JOB) and CHE-1955776 (LOB).

DATA AVAILABILITY STATEMENT

The data that supports the findings of this study are available within the article [and its Supplementary Material].

References

1. B. Grovem, M. Heyne, A.N. Mehta, H. Bender, T. Nuytten, J. Meersschaut, T. Conard, P. Verdonck, S. Van Elshocht, W. Vandervorst, S. De Gendt, M. Heyns, I. Radu, M. Caymax, and A. Delabie, *Chem. Mater.*, **29**, 2927-2938 (2017).
2. M.K.S. Bin Rafiq, N. Amin, H.F. Alharbi, M. Luqman, A. Ayob, Y. S. Alharthi, N.H. Alharthi, B. Bais, and M. Akhtaruzzaman*, Sci. Rep.* **10,** 771 (2020).
3. B. Liang and L. Andrews, *J. Phys. Chem. A*. **106,** 6945 (2002).
4. L.F. Tsang, M.-C. Chan, W. Zou, A.S.-C. Cheung, *J. Mol. Spectrosc*. **359,** 31 (2019).
5. J. Zhang, F. Fang, L. Zhang, D. Zhao, X. Ma, J. Yang, *J. Mol. Spectrosc*. **366**, 111223 (2019).
6. J.C. Harms, B.M. Ratay, K.N. Bales, J.J. O'Brien, and L.C. O'Brien, *J. Mol. Spectrosc.* **372,** 111349 (2020).
7. J.C. Harms, K.N. Bales, J.J. O'Brien, and L.C. O'Brien, *J. Mol. Spectrosc.* **374,** 111378 (2020).
8. J. L. Dunham, *Phys. Rev.* **41,** 721(1932).
9. J. Zhang, W. Zou, L. Zhang, D. Zhao, X. Ma, J. Yang. *J, Quant. Spectrosc. Radiat. Transfer.* **256,** 107314 (2020).
10. L.C. O'Brien, J.C. Harms, J.J. O'Brien, W. Zou, *J. Mol. Struc.* **1211,** 128024 (2020).
11. P.F. Bernath, *Spectra of Atoms and Molecules, 3rd Ed.* (Oxford University Press, New York, 2016).
12. V.M. Baev, T.P. Belikova, V.F. Gamalii, E.A. Sviridenkov, and A.F. Suchkov, *Sov. J. Quantum Electron*., **14**, 1596-1599 (1984).
13. Valery M. Baev, personal communication (November 2009).
14. W. Demtröder; Laser Spectroscopy, 2nd Edition (Springer, 1995)

15. PGOPHER, A Program for Simulating Rotational, Vibrational and Electronic Spectra, C. M. Western, *JQSRT* **186,** 221 (2017). doi:10.1016/j.jqsrt.2016.04.010. (version 10.1.182)

16. F. Kerber, G. Nave, and C.J. Sansonetti, *Astrophys. J., Suppl. Ser.* **178,** 374 (2008).

17. R. Ram, J. Liévin, and P.F. Bernath, *J. Mol. Spectrosc.* **256,** 216 (2009).

Conflict of Interest Statement

Analysis of the newly observed [15.05]$0^+ - X\,^3\Sigma^-(0^+)$ transition of WS observed using intracavity laser spectroscopy with Fourier-transform detection

Kristin N. Bales, Jack C. Harms, James J. O'Brien, and Leah C. O'Brien

The authors have no conflicts of interest regarding the research nor data that are contained in this manuscript.

Author Credit Statement

JMSP-D-20-: Analysis of the newly observed [15.05]0^+ – $X\,^3\Sigma^-(0^+)$ transition of WS observed using intracavity laser spectroscopy with Fourier-transform detection

Kristin N. Bales, Jack C. Harms, James J. O'Brien, and Leah C. O'Brien

Kristin N. Bales: Investigation, Formal analysis, Writing - Original Draft, Visualization

Jack C. Harms: Methodology, Investigation, Writing - Review & Editing, Validation, Software

James J. O'Brien: Conceptualization, Software, Validation, Resources, Data Curation, Visualization, Supervision, Funding acquisition

Leah C. O'Brien: Conceptualization, Methodology, Formal analysis, Resources, Writing - Review